



## Ballistic performance of composite armor impacted by 7.62 mm armor projectile

Apichart JINNAPAT<sup>1</sup>, Patchayapon DOUNGKOM<sup>2</sup>, Kritkeaw SOMTON<sup>3</sup>, and Kannigar DATERAKSA<sup>3,\*</sup>

<sup>1</sup> Department of Military and Aerospace Materials, Navaminda Kasatriyadhiraj Royal Thai Air Force Academy, 171/1 Phahonyothin Road, Khet Sai Mai, Bangkok, 10220, Thailand

<sup>2</sup> Faculty of Engineering and Technology, Pathumthani University, 140 Tiwanon Rd, Ban Klang, Amphoe Mueang, Pathum Thani, 12000, Thailand

<sup>3</sup> National Metal and Materials Technology Center (MTEC), National Science and Technology Development Agency (NSTDA) 111 Thailand Science Park, Phahonyothin Road, Khlong Nueng, Khlong Luang, Pathum Thani, 12120, Thailand

\*Corresponding author e-mail: kannigd@mtec.or.th

### Received date:

6 December 2022

### Revised date

29 March 2023

### Accepted date:

29 March 2023

### Keywords:

Alumina ceramic;  
Aluminum cubic lattice  
sandwich panels;  
Armor;  
Ballistic performance

### Abstract

The purpose of this study is to investigate the effectiveness of composite armor against 7.62 mm ballistic threats. A sandwich panel construction consisting of a 96% alumina ceramic strike face, an annealed aluminum alloy 7075 cubic lattice sandwich panel, and a thin aluminum backing plate were used to create hard armor. The ballistic test based on NIJ standard level III was performed using 7.62 mm × 51 mm NATO projectiles at an impact velocity of  $847 \pm 9.1 \text{ m}\cdot\text{s}^{-1}$ . The influences of the alumina strike face panel with thicknesses of 7, 10, and 14 mm on the ballistic performance were investigated. The results of the ballistic test suggest that hard armor designs can resist a ballistic impact of 7.62 mm × 51 mm NATO projectiles without penetrating them. With the increase in thickness of alumina ceramic tile, the deformation of the aluminum backing plate decreased. Furthermore, the annealed aluminum alloy 7075 cubic lattice sandwich panel could be able to absorb the residual kinetic energy of the projectile after it was eroded by the ceramic strike panel. The damaged targets after ballistic impact were presented. Collectively, these results indicate that the armor composites in this study may be used in military vehicle applications.

## 1. Introduction

Over the last several decades, a large number of studies have been carried out on lightweight armor systems and their ballistic performance. The armor systems are designed based on the requirements of performance, weight, application, and manufacturing ability. For military vehicle applications, the hard armor must be lightweight, cost-effective, and resistant of ballistic threats. A layered system consisting of a ceramic strike face with a composite or metal backing is widely used. Typical hard armor systems use a ceramic strike face backed by a ductile metal such as steel or aluminum. The ceramic armor layer is used to destroy the core of the projectile progressively as it attempts to penetrate the composite material through complex mechanisms, including fragmentation, wave scattering, and twinning [1-2] while the ductile material backing layer absorbs the residual impact energy of the bullet through plastic deformation [2-3].

The ceramic materials used as the armor strike face are alumina ( $\text{Al}_2\text{O}_3$ ), boron carbide ( $\text{B}_4\text{C}$ ), and silicon carbide ( $\text{SiC}$ ) due to their low density, high compressive strength, and hardness properties [4-7]. Out of the aforementioned materials, alumina continues to be extensively used as the preferred ceramic material in armor systems because it is inexpensive, good ballistic impact response, and can be manufactured by several processes [1].

Sandwich structures made of metal or an aluminum foam are relatively new materials because of their superior mechanical, thermal, and insulating qualities. It has been widely used for energy absorbers, bone substitute implants, aerospace, automotive, and defense industry applications [8-11]. For the ballistic impact application, the foam exhibits significant non-linear deformation and stress wave attenuation. The utilization of an aluminum or metal foam composite layer may lead to weight reduction, increased fuel efficiency, and overall cost effectiveness of the vehicle [12,13]. The ballistic performance of a metal foam-ceramic composite armor system was evaluated by Garcia-Avila *et al.* [14]. Composite metal foam (CMF) panels were manufactured using 2 mm diameter steel hollow spheres embedded in a stainless-steel powder matrix. Ballistic impact of 7.62 mm × 51 mm M80 and 7.62 mm × 63 mm M2 AP bullets were used to evaluate this armor system. The metal foam composite layer absorbed the initial kinetic energy of the bullet through plastic deformation. Marx *et al.* [15] studied the performance of composite metal foam armor against .50 caliber ballistic threats. A sandwich panel construction consisting of a ceramic faceplate, a CMF core, and a 7075-T6 aluminum backing plate were used to create hard armor plates. The CMF plate was 2 mm in diameter and 100 mm in wall thickness. The CMF layer was found to absorb 73% to 76% of the ball kinetic energy, or 69% to 79% of the AP round kinetic energy. Besides metal foam, lattice structures were also used

as energy absorption elements. The lattice structures fully controlled the internal morphology, causing high repeatability of the morphology and having higher mechanical properties than metal foam [16]. Hybrid composite armor was composed of aluminum honeycomb, which was between the strike face and the backing layer made of Dyneema® HB50 fabric composite. It showed a maximum reduction of the backing face signature of 40.8% in comparison to a baseline of the same weight, evaluated with the Level III NIJ 0101.06 body armor standard [17]. Body armor comprised adjoining hexagonal units which composed a regular diagonal lattice structure and a shell of Ti<sub>6</sub>Al<sub>4</sub>V showing good strength and high energy absorption. Energy absorption could be calculated from the stress-strain data in quasi-static compression tests [18].

This research was initiated in order to develop composite armor parts. The use of the annealed aluminum alloy cubic lattice sandwich panel as an intermediary layer between a ceramic strike face and the thin aluminum backing to create an efficient and lightweight hard armor solution. In this study, the 96% alumina ceramic thicknesses were studied for efficient ballistic protection with a constant thickness of annealed aluminum alloy 7075 lattice structure sandwich panels and aluminum alloy 7075 backing plates. The energy absorption performance of the annealed aluminum alloy 7075 lattice structure sandwich panel and as cast sample was evaluated via three-point bending. The efficient ballistic impact and damage zone of the target were discussed.

## 2. Experimental

### 2.1 The armor systems

Hexagonal tiles made of 96% alumina, sandwich panels with a lattice structure made of annealed aluminum alloy 7075, and commercial aluminum alloy 7075 backing plates were utilized to create the composite armor. In this study, the armor alumina ceramic used as strike panels is made from 96 wt% alumina powder (A-32, Nicho, Thailand), 1.5 wt% clay powder (Compound Clay Co., Ltd., Thailand), 2.5 wt% dolomite powder (Compound Clay Co., Ltd., Thailand), and 2 wt% polyvinyl alcohol (PVA, Mitsubishi Chemical Corporation) organic binder. The mixed powders were milled in water for 24 h using an alumina media ball. The spray dryer was used to prepare granules with inlet and outlet temperatures of 330°C and 105°C, respectively. Alumina tiles were prepared by pressing 96% alumina granules into hexagonal mosaics of various thicknesses of 7, 10, and 14 mm. The tiles were sintered at 1650°C for 2 h at a heating rate of 5°C·min<sup>-1</sup>.

For the annealed aluminum alloy 7075 lattice structure sandwich panel model prepared by using SolidWorks 2018 (SOLIDWORKS 2018, SolidWorks EDU Edition NETWORK-Campus, Serial Number: 970014865465811F9D2J9K4) as shown in Figure 1. Individual cells were cubic frameworks. The cell sizes were 3 mm × 3 mm with a strut thickness of 1 mm. The skin thickness was 1.5 mm on the top and bottom faces, which enclosed the lattice core. The dimensions of the sandwich structure were 50 mm × 22 mm × 100 mm.

Figure 2 shows the polymer lattice structure sandwich panels which were 3D-printed in polylactic acid (PLA) by fused filament fabrication using a FLASHFORGE 3D printer (FLASHFORGE CREATOR PRO, China) without requiring support materials for

a fast-manufacturing process. The metallic lattice structure sandwich panel was then created by pouring molten aluminum alloy 7075 into the plaster mold template. The aluminum alloy 7075 was melted (700°C) in SiC crucible inside a furnace. The melt was kept isothermal at 700°C for 10 min for homogenization. Then, the melt was cast in vacuum (P=-62 cm Hg) into the pre-heated plaster mold (400°C). The plaster mold was submerged in water to separate it from the cast sample after a 10 min solidification period. The cast sample was heat treatment, annealing, to 470°C, soaking at this temperature for 3 h, and then furnace cooled. The investment cast aluminum alloy 7075 lattice structure with a cubic unit cell was created using a 3D-printed polymer pattern as a template shown in Figure 3.

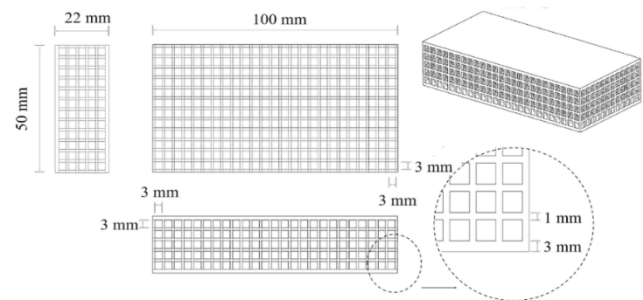


Figure 1. The samples are modeled using SolidWorks 2018.

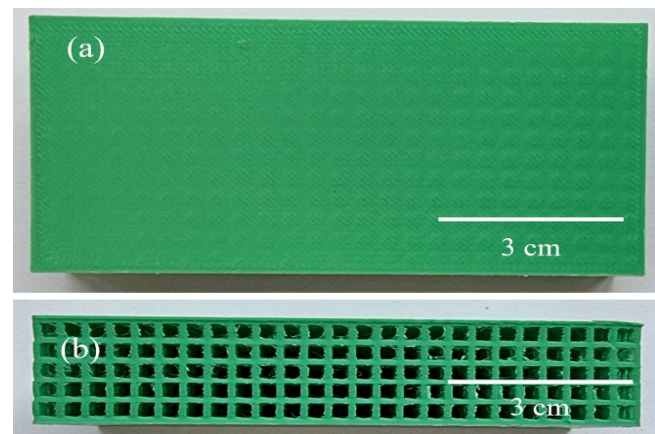


Figure 2. The polymer lattice structure sandwich panels by 3D-printed in polylactic acid fused filament fabrication (a) top view and (b) side view.

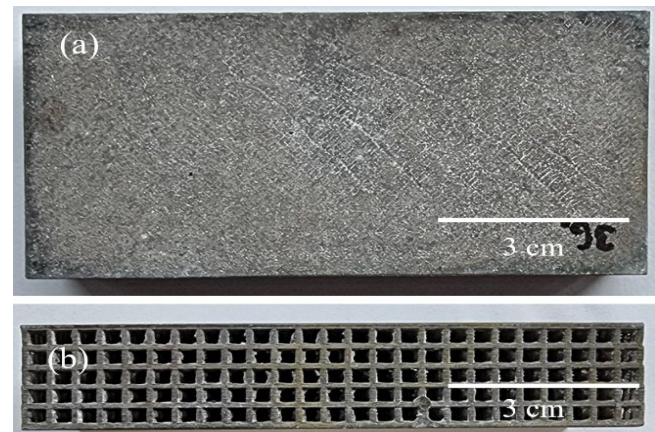
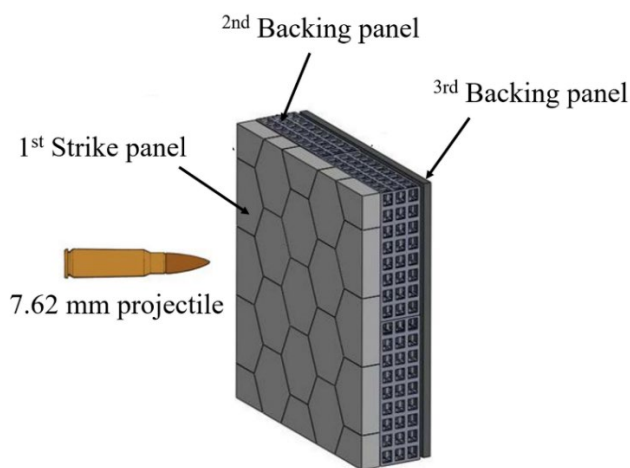


Figure 3. As cast aluminum lattice structure sandwich panel modeled with a cubic unit cell (a) top view and (b) side view.



**Figure 4.** Schematic diagram of the designed composite armor.

A 22 mm annealed aluminum alloy 7075 cubic lattice sandwich panel was sandwiched between the alumina ceramic strike face and the 6 mm aluminum alloy 7075 backing plate for the designed composite armor (Figure 4). The mixed ratio of 5 wt% epoxy resin (Buehler Ltd.) to 1 wt% hardener (Buehler Ltd.) was used to adhere to the armor layer, which was covered with fabric to guard against bullet shrapnel. The armor configurations in this study are shown in Table 1. The total areal weight density of the three armor systems was 6.0, 7.2, and 8.7 g·cm<sup>-2</sup>.

## 2.2 Ballistic test

The ballistic testing was performed according to U.S. Military and National Institute of Justice (NIJ) standards. The testing was at level 3, which is 7.62 mm NATO ammunition, and was conducted at a velocity of  $847 \pm 9.1$  m·s<sup>-1</sup>. The target and the test barrel were separated by 15 meters. A single shot was fired at the center of each armor with zero-degree obliquity. The average values of three test samples are reported.

## 2.3 Characterization

For alumina ceramics, the apparent density and porosity of sintered samples were measured by Archimedes' principle. The three-point bending was determined using a universal testing machine (Instron 8872) with a span of 20 mm and a crosshead speed of 0.5 mm·min<sup>-1</sup>. The hardness was measured on the Vickers hardness tester (Zwick 3212) using a 2 kg load. The elastic properties were measured by

an ultrasonic pulse-echo technique (Grindosonic MK51). After the ballistic tests, the damage zones of the ceramic tiles, including ceramic fragmentation were observed by SEM scanning electron microscopy (SEM: JOEL, JSM-6480LV, Japan) operated at 20 kV in secondary electron mode and optically.

For the aluminum alloy 7075 lattice sandwich panel and the aluminum alloy 7075 backing plate, the chemical compositions were determined using Micro-Energy Dispersive X-ray Fluorescence Spectrometer (EDAX Inc.). The density was calculated from the ratio between their weight and volume. The three-point bending test of the aluminum alloy 7075 lattice structure sandwich panel was determined using a universal testing machine (Instron model 8872). The quasi-static load was applied at a crosshead speed of 0.5 mm·min<sup>-1</sup> with a preload of 1 N. The hardness of the aluminum alloy 7075 backing plate was determined by Rockwell tester (Wilson 574) with a 10 kgf load and dwell time of 3.5 s. The morphology of the microstructures of heat treated and as cast samples was then characterized by optical microscopy (ZEISS/Axiotech) after etching with 4 mL HF, 6 mL HCl, 8 mL HNO<sub>3</sub>, and 82 mL water.

## 3. Results and discussion

### 3.1 The chemical composition, physical, and mechanical properties of samples

Table 2 displays the physical and mechanical characteristics of ceramics made from 96% alumina. The apparent density of the 96% alumina ceramic is 3.83 g·cm<sup>-3</sup>, and its flexural strength, hardness, and Young's modulus are 311 MPa, 1252 kg·mm<sup>-2</sup>, and 305 GPa, respectively.

The chemical analysis of aluminum alloy 7075 for the cubic lattice sandwich panel and aluminum alloy 7075 for the backing panel used for this study is shown in Table 3. It was found that the aluminum alloy 7075 mainly consisted of Al, Zn, Mg, and Cu. Table 4 shows the physical and mechanical properties of annealed aluminum alloy 7075 cubic lattice sandwich panel and the aluminum alloy 7075 backing plate. The cubic lattice sandwich panel made of the aluminum alloy 7075 has a density of 0.8 g·cm<sup>-3</sup> and a flexural strength of 15 MPa. The density and hardness for the aluminum alloy 7075 backing plate are 2.8 g·cm<sup>-3</sup> and 90 HRB, respectively.

The three-point bending properties of a sandwich panel made of as cast and annealed aluminum alloy 7075 lattice structure are shown in Figure 5. The energy absorption of heat-treated aluminum alloy 7075 lattice structure shows a larger value of bending deflection than as cast sample.

**Table 1.** Armor configurations in this study.

Configuration	Alumina thickness (mm)	Annealed aluminum alloy 7075 lattice structure thickness (mm)	Aluminum alloy 7075 backing plate thickness (mm)	Areal density (g·cm <sup>-2</sup> )
I	7.0 ± 0.1	22.0 ± 0.1	6.0 ± 0.1	6.0 ± 0.1
II	10.0 ± 0.2	22.0 ± 0.1	6.0 ± 0.1	7.2 ± 0.1
III	14.0 ± 0.2	22.0 ± 0.1	6.0 ± 0.0	8.7 ± 0.1

**Table 2.** Physical and mechanical properties of 96% alumina used in this study.

Properties	Value
Apparent density, g·cm <sup>-3</sup>	3.83 ± 0.03
Bulk density, g·cm <sup>-3</sup>	3.70 ± 0.03
Open density, %	3.44 ± 0.13
Flexural strength, MPa	311 ± 25
Vickers hardness, Kg·mm <sup>-2</sup>	1252 ± 135
Young modulus, GPa	305 ± 1

**Table 3.** Chemical composition of aluminum alloy 7075.

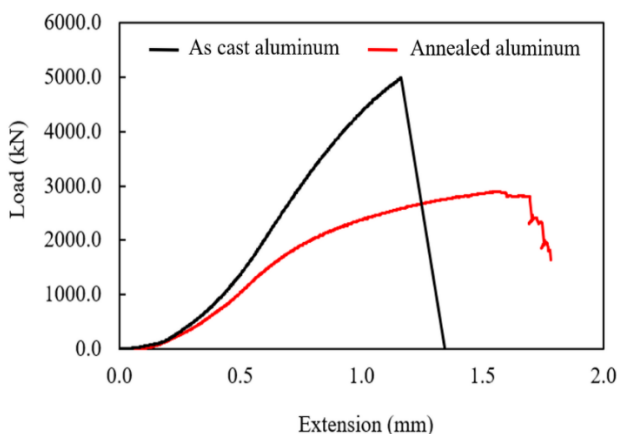
Material	Composition (wt%)					
	Zn	Mg	Cu	Cr	Fe	Al
Aluminum alloy 7075 for cubic lattice sandwich panel	6.8	2.7	1.7	0.2	0.1	Balance
Aluminum alloy 7075 for backing panel	7.3	2.7	1.4	0.2	0.2	Balance

**Table 4.** Physical and mechanical properties of annealed aluminum alloy 7075 cubic lattice sandwich panel and the aluminum alloy 7075 backing plate used in this study.

Properties	Annealed aluminum alloy 7075 cubic lattice sandwich panel	Aluminum alloy 7075 backing plate
Bulk density, g·cm <sup>-3</sup>	0.8	2.8
Flexural strength, MPa	15 ± 0.1	-
Young's modulus (GPa)	13 ± 0.6	-
Hardness, (Rockwell, HRB)	-	90 ± 0.6

**Table 5.** Ballistic testing results for armor composites with different ceramic thicknesses as a front layer.

Configuration	Ceramic thickness (mm)	Impact velocity (m·s <sup>-1</sup> )	Aluminum alloy 7075 backing plate deformation (mm)	Penetration (CP/PP)
I	7.0 ± 0.1	845.4 ± 2.2	6.4 ± 0.6	PP
II	10.0 ± 0.2	842.7 ± 2.2	2.5 ± 0.5	PP
III	14.0 ± 0.2	842.3 ± 1.8	0.0	PP

**Figure 5.** Bending properties of a sandwich panel made of as cast and annealed aluminum alloy 7075 lattice structure.

### 3.2 Ballistic performance of armor systems

Table 5 shows the results of the ballistic tests for armor composites with different ceramic thicknesses as a strike face. The results of

the ballistic impacts against the armor composite are analyzed and classified as either complete penetration (CP) or partial penetration (PP). When the armor is able to stop the bullet, the test is classified as PP, but when the projectile creates a hole large enough to pierce the armor, it is classified as CP. The target defeated the projectile. All armor systems can protect against 7.62 mm projectiles without allowing penetration under the impact of the projectiles. The bullet shots were stopped by the aluminum backing plate.

Figure 6 illustrates the damage of the front views of the alumina with thicknesses of 7, 10, and 14 mm after the ballistic test. The alumina tile impacted by the projectile was completely fragmented into different sizes, ranging from big chunks to fine powder, while its neighboring tiles had only a few cracks. The compression wave created on the impact surface of ceramic under high impact loading causes damage to the material [19]. Moreover, it was found that some ceramic tiles separated upon projectile impact due to weak adhesive layer.

The images of the 22 mm annealed aluminum alloy 7075 cubic lattice sandwich panel after ballistic testing are displayed in Figure 7. The sandwich panel interlayer of composite armor composed of a light-weight core connects the solid facesheets, providing a high bending and buckling resistance and excellent shear stiffness and

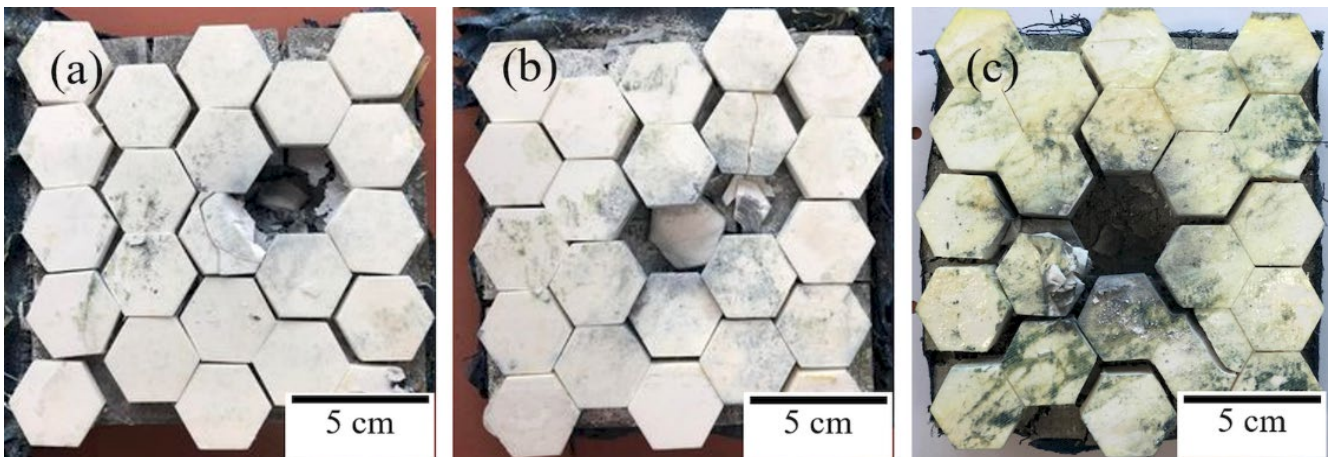
energy absorption capability. Cellular cores carry transverse shear and compression loads and solid facesheets carry in-plane load and flexure [20]. The sandwich panel interlayer absorbed residual compressive waves, as well as the kinetic energy of the bullet from strike panel through the plastic deformation of it [14].

Figure 8 displays the front, rear, and side views of the aluminum backing plate using a 7, 10, and 14 mm alumina strike panel. As shown in Figure 8(a-c), it is obvious that the diameter of the damaged area on the front view of the aluminum backing plate using a 7 mm alumina strike panel was measured to be 5 cm, which was greater than the diameter of the damaged area (3 cm) measured for the aluminum backing plate using a 10 mm alumina strike panel. There was no damage area on the surface of the aluminum alloy 7075 backing plate when using a 14 mm alumina strike panel. The damaged area on the rear view of the aluminum alloy 7075 backing plate is shown in Figure 8(d-f). It was found that the aluminum alloy 7075 backing plate dissipates the remaining projectile energy through plastic deformation. Microcracks can be observed on the back of the impact point when using 7 mm alumina strike panel. There was no appreciable plastic deformation zone observed at the aluminum alloy 7075 backing plate using 14 mm alumina as the front layer. The high deformation peak was measured on the side view of the back panels, as seen in

Figure 8(g-i). The highest deformation peak (7 mm) was observed in the aluminum alloy 7075 backing plate using 7 mm alumina strike panel. There was no deformation peak formed around the impact axis of the projectile for the aluminum alloy 7075 backing plate using a 14 mm alumina strike panel. The difference may be explained by the ceramic thickness of the strike panel, which effectively fragments the projectile and significantly reduces the impacted energy. As the alumina ceramic front layer thickness is increased, the projectile's interaction time can be prolonged, resulting in greater energy loss through effective blunting, eroding, and breaking [21].

### 3.3 Microstructure of alumina after ballistic test

Figure 9 shows SEM images of the fracture surface of alumina ceramic after ballistic testing. The SEM images show that the fragmented spalling grains are evident on the surface, which offers resistance to penetration. Ceramic fragmentation under ballistic impact favors the dissipation of energy. The microstructure of all samples show very similar characteristics. The fracture is an intergranular fracture along grain boundaries, which is consistent with the author's research [22,23]. Intergranular cracking could be beneficial to the ballistic performance of the ceramic.



**Figure 6.** Photographs the damage of the front view of the alumina with a thickness of (a) 7 mm, (b) 10 mm, and (c) 14 mm after ballistic testing.

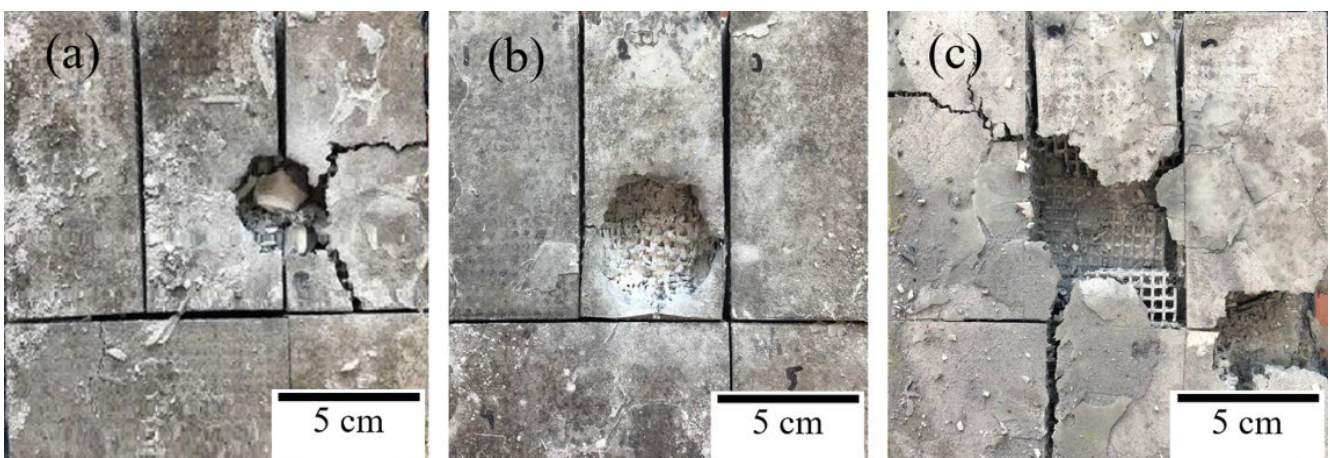


**Figure 7.** Photographs of the front view of a 22 mm annealed aluminum alloy 7075 cubic lattice sandwich panel after ballistic testing using alumina strike panel with a thickness of (a) 7 mm, (b) 10 mm, and (c) 14 mm.

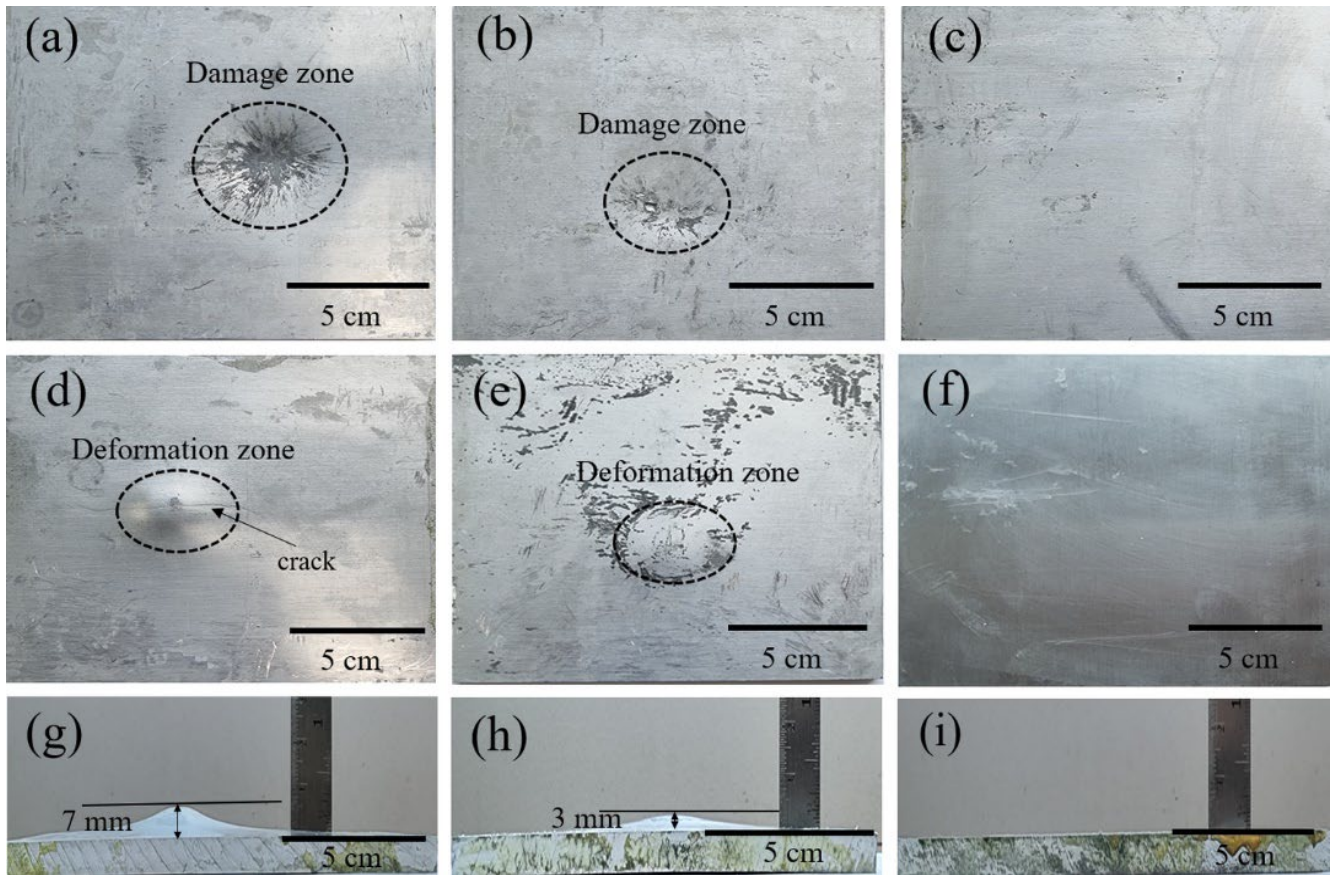


**Figure 8.** Photographs of the front (a, b, c), rear (d, e, f), and side views (g, h, i) of the 6 mm aluminum alloy 7075 backing plate after ballistic testing using alumina strike panel with the thickness of (a, d, g) 7 mm, (b, e, h) 10 mm, and (c, f, i) 14 mm.

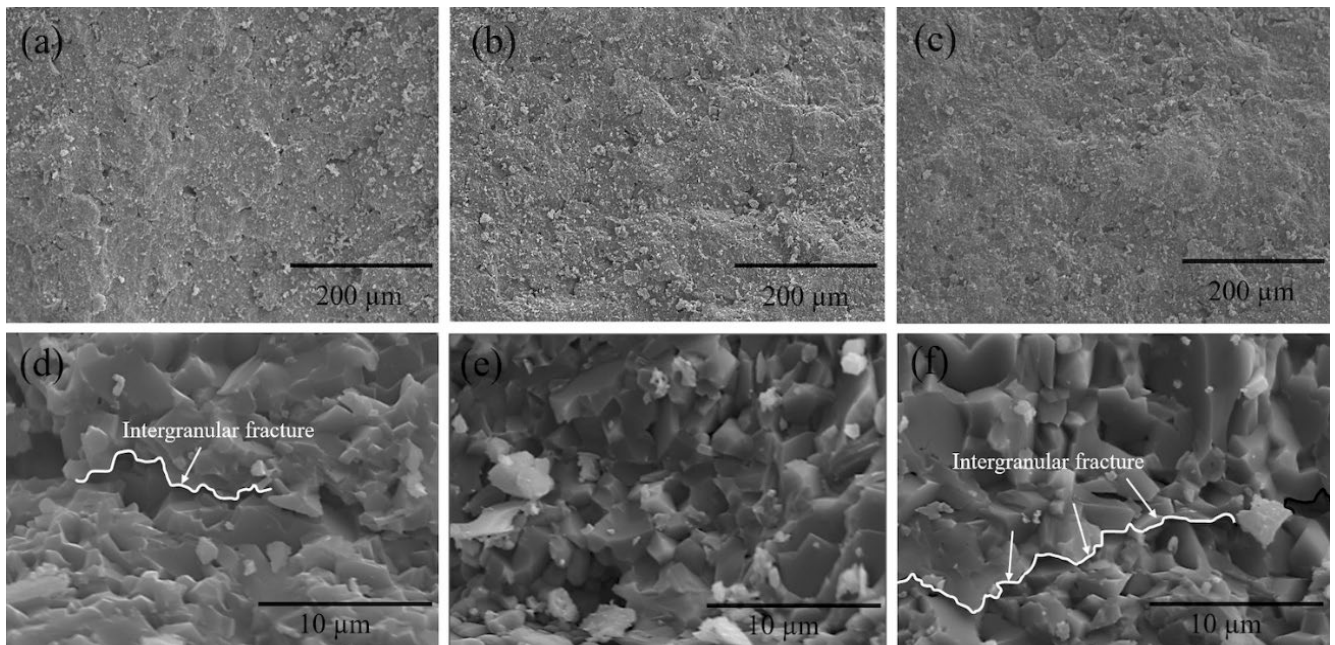


**Figure 9.** The SEM micrographs of the fracture regions of the alumina samples with the thickness of (a, d) 7 mm, (b, e) 10 mm, and (c, f) 14 mm with magnification of 200 and 5000X after the ballistic testing.

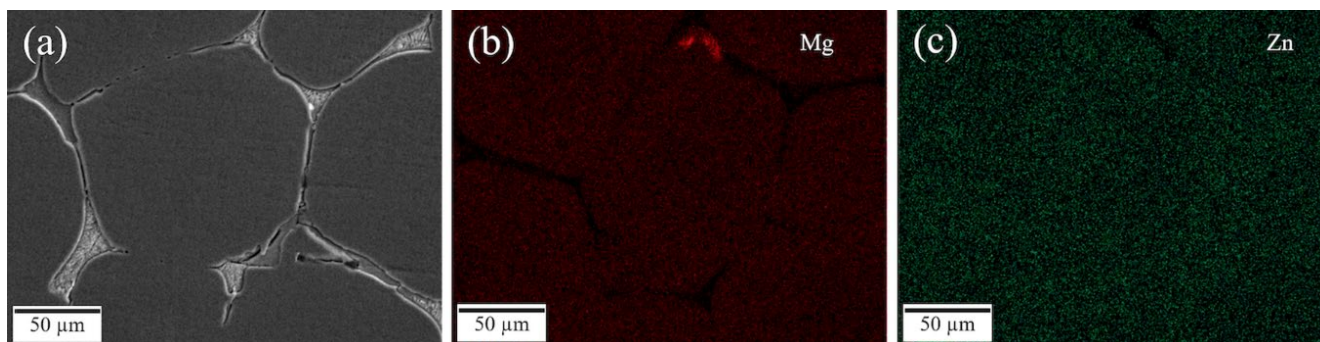


**Figure 10.** Microstructure of (a) the gradually cooled as-cast 7075 aluminum alloy and (b, c) EDX analysis showing distribution map of Mg and Zn in the representative SEM respectively resulting microsegregation of  $MgZn_2$  in aluminum matrix.

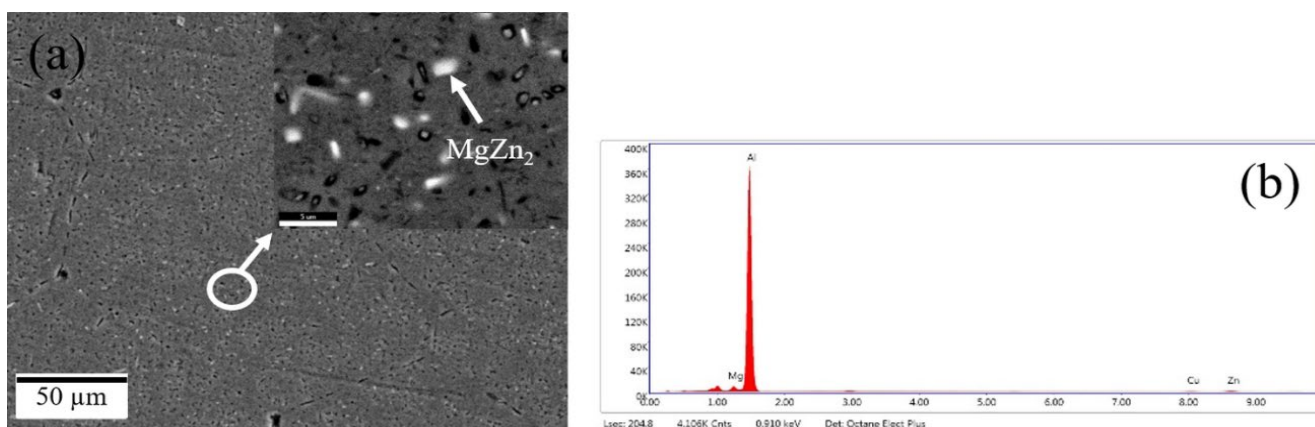


**Figure 11.** (a) Microstructure of the annealed 7075 aluminum alloy showing coarse grains  $MgZn_2$  phase in the aluminum matrix. (b) The EDS spectra results of the  $MgZn_2$  phases.

### 3.4 Aluminum lattice structure sandwich panel deformation

Deformation of as cast sample (non-heat treatment) showed brittle characteristic but annealed sample (heat treatment) showed ductile characteristic, the more value of bending deflection. Even though the brittle has higher yield and bending strengths, it has a lower deflection than the ductile one, annealed sandwich panel as it can be seen in Figure 5. Microstructure of gradually cooled as-cast aluminum alloy 7075 showed microsegregation of  $MgZn_2$  in aluminum matrix being susceptible to embrittlement. The microsegregation of  $MgZn_2$  shown in EDX analysis showing distribution map of Mg and Zn in the representative SEM image as shown in Figure 10. However, the microstructure of annealed sample showed coarse grains of  $MgZn_2$  phase which is non-uniformly distributed in the aluminum matrix as shown in Figure 11. This promotes the formation of small hard precipitates which interfere with the motion of dislocations and improve its mechanical properties. Annealing samples are improved impact strength and ductility for applications involving toughness and ductility works [24]

## 4. Conclusion

The ballistic efficiency of armor composites consisting of a 96% alumina ceramic strike panel bonded with the 22 mm annealed aluminum alloy 7075 cubic lattice sandwich panel interlayer and the aluminum alloy 7075 backing plate has been investigated. The thickness of the

strike panel indicates an ability to destroy the projectile into fragments with no failure formed on the back panel. Likewise, the annealed 22 mm aluminum alloy 7075 cubic lattice sandwich panel could result in ballistic impact response, particularly in terms of ductile material. Collectively, the results indicate that composite hard armor designs could protect against the perforation of 7.62 mm NATO ammunition with an impact velocity of  $847 \pm 9.1 \text{ m}\cdot\text{s}^{-1}$ . Utilization of the 14 mm alumina as a strike panel bonded with the 22 mm aluminum alloy 7075 cubic lattice sandwich panel and the 6 mm aluminum alloy 7075 backing plate show the highest ballistic performance. However, the armor design with the 10 mm alumina thickness combined with the aluminum lattice structure sandwich panel with the thickness of the 22 mm and the 6 mm aluminum alloy 7075 thickness may be suitable for use in composite hard armor applications, especially considering that the areal weight density was measured to be  $7.2 \text{ g}\cdot\text{cm}^{-2}$ . In summary, the armor design of this study assures the potential of lightweight armor for future armored vehicles.

## Acknowledgements

The authors would like to thank the Department of Military and Aerospace Materials, Navaminda Kasatriyadhiraj Royal Thai Air Force Academy, for providing funding for this project. Highly thankful to the National Metals and Materials Technology Center (MTEC) for the characterization equipment.

## References

- [1] E. Medvedovski, "Ballistic performance of armour ceramics: Influence of design and structure. Part 1," *Ceramics International*, vol. 36, no. 7, pp. 2103-2115, 2010.
- [2] K. Dateraksa, K. Sujirote, R. McCUISTON, and D. Atong, "Ballistic performance of ceramic/S<sub>2</sub>-glass composite armor," *Journal of Metals, Materials and Minerals*, vol. 22, no. 2, pp. 33-39, 2012.
- [3] M. V. Silva, D. Stainer, H. A. Al-Qureshi, O. R. K. Montedo, and D. Hotza, "Alumina-based ceramics for armor application: mechanical characterization and ballistic testing," *Journal of Ceramics*, 2014.
- [4] W. Liu, Z. Chen, X. Cheng, Y. Wang, A. R. Amankwa, and J. Xu, "Design and ballistic penetration of the ceramic composite armor," *Composites Part B: Engineering*, vol. 84, pp. 33-40, 2016.
- [5] D. Hu, Y. Zhang, Z. Shen, and Q. Cai, "Investigation on the ballistic behavior of mosaic SiC/UHMWPE composite armor systems," *Ceramics International*, vol. 43, no. 13, pp. 10368-10376, 2017.
- [6] I. G. Crouch, G. Appleby-Thomas, and P. J. Hazell, "A study of the penetration behaviour of mild-steel-cored ammunition against boron carbide ceramic armours," *International Journal of Impact Engineering*, vol. 80, pp. 203-211, 2015.
- [7] Z. Yin, J. Yuan, M. Chen, D. Si, and C. Xu, "Mechanical property and ballistic resistance of graphene platelets/B<sub>4</sub>C ceramic armor prepared by spark plasma sintering," *Ceramics International*, vol. 45, no. 17, pp. 23781-23787, 2019.
- [8] L. Peroni, M. Avalle, and M. Peroni, "The mechanical behaviour of aluminium foam structures in different loading conditions," *International Journal of Impact Engineering*, vol. 35, no. 7, pp. 644-658, 2008.
- [9] B. A. Gama, J. W. Gillespie, T. A. Bogetti, and B. K. Fink, "Innovative design and ballistic performance of lightweight composite integral armor," *SAE transactions*, vol. 110, no. 2, pp. 32-41, 2001.
- [10] B. A. Gama, T. A. Bogetti, B. K. Fink, C. J. Yu, T. D. Claar, H. H. Eifert, and J. W. Gillespie Jr, "Aluminum foam integral armor: a new dimension in armor design," *Composite Structures*, vol. 52, pp. 381-385, 2001.
- [11] J. Banhart, F. García-Moreno, K. Heim, and H. W. Seeliger, "Light-weighting in transportation and defence using aluminium foam sandwich structures," *In Light Weighting for Defense, Aerospace, and Transportation*, pp. 61-72, 2019.
- [12] A. Rabiei, L. Vendra, N. Reese, N. Young, and B. P. Neville, "Processing and characterization of a new composite metal foam," *Materials Transactions*, vol. 47, no. 9, pp. 2148-2153, 2006.
- [13] B. P. Neville, and A. Rabiei, "Composite metal foams processed through powder metallurgy," *Materials & Design*, vol. 29, no. 2, pp. 388-396, 2008.
- [14] M. Garcia-Avila, M. Portanova, and A. Rabiei, "Ballistic performance of a composite metal foam-ceramic armor system," *Procedia Materials Science*, vol. 4, pp. 151-156, 2014.
- [15] J. Marx, M. Portanova, and A. Rabiei, "Ballistic performance of composite metal foam against large caliber threats," *Composite Structures*, vol. 225, p. 111032, 2019.
- [16] O. Al-Ketan, R. K. A. Al-Rub, and R. Rowshan, "The effect of architecture on the mechanical properties of cellular structures based on the IWP minimal surface," *Journal of Materials Research*, vol. 33, no. 3, pp. 343-359, 2018.
- [17] A. Bhat, "Honeycomb in hybrid composite armor resisting dynamic impact," *Doctoral dissertation, Oklahoma State University*, 2015.
- [18] A. du Plessis, and C. Broeckhoven, "Metal body Armour: biomimetic engineering of lattice structures," *19<sup>th</sup> Annual International RAPDASA conference*, 2018.
- [19] D. Hu, Y. Zhang, Z. Shen, and Q. Cai, "Investigation on the ballistic behavior of mosaic SiC/UHMWPE composite armor systems," *Ceramics International*, vol. 43, no. 13, pp. 10368-10376, 2017.
- [20] H. Y. Sarvestani, A. H. Akbarzadeh, A. Mirbolghasemi, and K. Hermenean, "3D printed meta-sandwich structures: Failure mechanism, energy absorption and multi-hit capability," *Materials & Design*, vol. 160, pp. 179-193, 2018.
- [21] G. H. Liaghat, H. Shanazari, M. Tahmasebi, A. Aboutorabi, and H. Hadavinia, "A modified analytical model for analysis of perforation of projectile into ceramic composite targets," *Journal of Composite Materials*, vol. 3, pp. 17-22, 2013.
- [22] K. Sujirote, K. Dateraksa, and N. Chollacoop, "Practical requirements for alumina armor systems," *American Ceramic Society Bulletin*, vol. 86, no. 3, pp. 20-25, 2007.
- [23] F. De Oliveira Braga, F. S. da Luz, S. N. Monteiro, and É. P. Lima Jr, "Effect of the impact geometry in the ballistic trauma absorption of a ceramic multilayered armor system," *Journal of Materials Research and Technology*, vol. 7, no. 4, pp. 554-560, 2018.
- [24] A. D. Isadare, B. Aremo, M. O. Adeoye, O. J. Olawale, and M. D. Shittu, "Effect of heat treatment on some mechanical properties of 7075 aluminium alloy," *Materials Research*, vol. 16, pp. 190-194, 2013.